

A Low-Speed Control Module for a Streamlined AUV

Christopher L. Nickell and Craig A. Woolsey
Department of Aerospace and Ocean Engineering
Virginia Polytechnic and State University
Blacksburg, Virginia 24061
Email: {cnickell, cwoolsey}@vt.edu

Daniel J. Stilwell
Bradley Department of Electrical and Computer Engineering
Virginia Polytechnic and State University
Blacksburg, Virginia 24061
Email: stilwell@vt.edu

Abstract—Streamlined autonomous underwater vehicles (AUVs) are typically designed to operate at a nominal speed. Control surfaces are sized to meet control requirements near this operating condition. Occasionally, the need arises for a vehicle to operate at a lower speed, for example, to perform an inspection task. Because hydrodynamic forces and moments decrease quadratically with speed, there is generally some minimum speed below which a streamlined AUV can not operate. If the vehicle is slightly buoyant, for example, it may be incapable of generating sufficient down-force to maintain depth. This paper describes the use of a moving mass actuator (MMA) module to augment control of an existing streamlined AUV in order to obtain a lower minimum operating speed. In some scenarios, as described in the paper, the MMA may be combined with a fixed wing to generate additional lift. The results of analysis include sizing guidelines for control surfaces and MMA modules and a technique for estimating the minimum controllable speed.

I. INTRODUCTION

Streamlined autonomous underwater vehicles (AUVs) are designed to swim efficiently over long distances. Moreover, even though additional power is required to maintain depth, AUVs are typically trimmed to be slightly buoyant or slightly heavy. If the system fails, the vehicle will then either rise to the surface or sink to the bottom. Buoyant or heavy streamlined AUVs maintain depth through some combination of propulsion and lift generated by the hull. Both components require the vehicle to travel at a nonzero pitch angle, which a nonzero control moment. In conventional vehicles, the control moment is generated by control surfaces. Both the control moment and the lift generated by the body vary quadratically with speed so that, at some minimum speed, the body is unable to maintain depth.

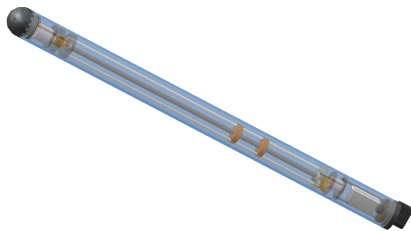


Fig. 1. One degree of freedom MMA.

A moving mass actuator (MMA) can provide control mo-

ments that are independent of vehicle speed. In this paper, we consider the problem of controlling longitudinal motion of a conventional streamlined AUV at low speed, where stern planes are prone to saturate. Consider the modular, one degree of freedom MMA shown in Fig. 1. When secured below a streamlined vehicle, such as the Virginia Tech Miniature AUV (VTMAUV) shown in Fig. 2, the actuator provides a constant gravitational pitch moment that depends only on the size and longitudinal location of the moving mass. A properly sized MMA can therefore extend the lower speed limit without greatly diminishing the vehicle's efficiency at its nominal speed.

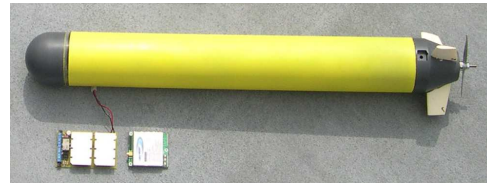


Fig. 2. Virginia Tech Miniature AUV [3].

A two degree of freedom MMA can provide control in pitch and roll. For a neutrally buoyant vehicle, for example, a two degree of freedom MMA would enable tilt control in hover. Another application is demonstrated by a new class of AUV, the buoyancy-driven underwater glider. Power storage is the essential limitation for AUVs. Because conventional marine propulsors are too inefficient for long-term, battery-powered operation, underwater gliders have begun to play a crucial role in long-term oceanographic monitoring [1]. A key advantage of moving mass actuators in this application is their intrinsic robustness. Since the actuators are housed internally, they are not subject to corrosion and biological fouling. Thanks to their extreme efficiency and robustness, gliders have already demonstrated endurance of months; deployments exceeding one year are not unrealistic. A thorough review of existing buoyancy driven glider technology is given in [7], along with design guidelines and quantitative comparisons to other flying vehicles and creatures. An excellent discussion of modeling and control design is given in [4].

The concept of buoyancy-driven gliding raises another question related to low-speed control of conventional streamlined

AUVs: When should one add a wing? A wing provides a greater lift force at smaller angles of attack, allowing a heavy or buoyant vehicle to maintain depth at lower speeds, although it also produces greater drag. To determine whether a wing is necessary and, if so, what its dimensions should be, one must consider the vehicle's hydrodynamics, its submerged weight, and the desired speed. Section II discusses wing sizing for a streamlined AUV.

Alternative methods for attitude control at low speed include additional fixed thrusters, super-articulated fins, or internal rotors such as reaction wheels or control moment gyroscopes. Additional thrusters are commonly used on remotely operated vehicles, however they are subject to fouling and corrosion and can add significantly to a vehicle's drag at higher speeds. Super-articulated fins have been demonstrated for control in hover [9], [5], however these actuators are also subject to fouling and corrosion. Reaction wheels can be used to control a vehicle at low speed, but they consume considerable power and volume and are subject to saturation [11]. Each of these moment actuators requires continuous power, unlike a MMA which exerts a gravitational moment.

Increasingly common among streamlined AUVs is vectored thrust propulsion. A vectored thruster can generate pitch and yaw moments which are more or less independent of speed, although it can not be used for roll control. As is true for stern planes, the off-axis force generated by a vectored thruster is opposite the direction of desired force. (For example, in order to pitch nose down to generate a downward body lift force, the stern planes or vectored thruster must generate a local upward force.) Thus, some of the thrust which could otherwise contribute to maintaining depth instead makes the problem more difficult. For a vehicle with a fixed thruster and a MMA, all of the thrust acts in the desired direction in trimmed flight.

II. LONGITUDINAL STATICS AND COMPONENT SIZING

Here, we consider longitudinal motion of a streamlined AUV with a MMA. We fix a reference frame in the body at the center of buoyancy (CB), assumed to be located at the geometric center. The body x_B axis is aligned with the hull's axis of symmetry and the body z_B axis points down through the belly. The y_B axis completes the right-handed triad. The body center of gravity (less the contribution of the moving mass) is located at the point r_{cg} with respect to the body frame; the mass of the body less the point mass is m_b . The point mass m_p is located at the point r_p .

Fig. 3 depicts a longitudinal free body diagram for an AUV with a fixed tail. To determine the potential benefit of a fixed wing, we assume that one is attached to the vehicle such that the wing aerodynamic center is aligned with the CB. (The aerodynamic center is the point about which the wing moment does not vary with the angle of attack.) Important length ratios for the vehicle shown in Fig. 4 are the fineness ratio $f = \frac{2r}{L}$ and the ratio $\gamma = \frac{s}{r} \geq 1$.

The normal force and pitching moment coefficients for a

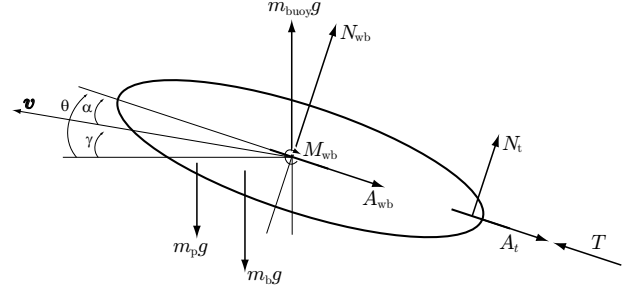


Fig. 3. Longitudinal free body diagram.

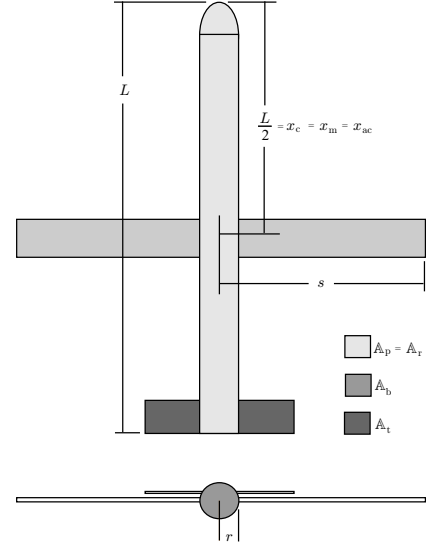


Fig. 4. Reference lengths and areas.

slender body with a constant cross-sectional shape are [8]

$$C_{N_{hull}} = \frac{A_b}{A_r} \left(\frac{1}{\gamma^2} + \gamma^2 - 1 \right) \sin 2\alpha \cos \frac{\alpha}{2} + \eta C_{d_n} \frac{A_p}{A_r} \left(\frac{3}{2}\gamma - \frac{1}{2} \right) \sin^2 \alpha \quad (1)$$

$$C_{m_{wb}} = \left(\frac{\nabla - A_b(l - x_m)}{A_r X} \right) \left(\frac{1}{\gamma^2} + \gamma^2 - 1 \right) \sin 2\alpha \cos \frac{\alpha}{2} + \eta C_{d_n} \frac{A_p}{A_r} \left(\frac{x_m - x_c}{X} \right) \left(\frac{3}{2}\gamma - \frac{1}{2} \right) \sin^2 \alpha \quad (2)$$

In these expressions, ∇ represents the vehicle volume and η represents an empirical factor (assumed here to be one) which accounts for cross-flow drag. The actual force and moment are

$$N_{hull} = C_{N_{hull}}(\alpha) P_{dyn} A_r \quad (3)$$

$$M_{wb} = C_{m_{wb}}(\alpha) P_{dyn} A_r L \quad (4)$$

where

$$P_{dyn} = \frac{1}{2} \rho V^2$$

is the dynamic pressure. Because the dynamic pressure varies quadratically with the water-relative speed V , the hydrodynamic force and moment vanish at very low speeds. By increasing the wing size (represented by the factor γ), one

may increase the lift force at lower speeds to aid in maintaining depth. At zero water-relative speed, however, only a vertical thruster or a buoyancy control device will allow a vehicle to maintain a fixed depth.

The moment coefficient in equation (2) represents a destabilizing pitching moment due to the wing and body. The effect may be offset by including properly sized stern planes. Servo-actuated stern planes are the conventional means of pitch actuation for streamlined AUVs. The tail moment contribution scales linearly with the area ratio $\frac{A_t}{A_r}$ so that

$$C_N = C_{N_{\text{hull}}} + \frac{A_t}{A_r} C_{N_t} \quad (5)$$

where, for a flat plate [6],

$$C_{N_t} = \frac{1}{0.222 + \frac{0.283}{\sin \alpha}}. \quad (6)$$

The axial force coefficient for the tail is

$$C_{A_t} = C_{D_{f_0}} \cos^2 \alpha_f. \quad (7)$$

The term $C_{D_{f_0}}$ in (7) is the zero angle of attack tail drag coefficient for the tail and α_f is the stern plane angle of attack, including the commanded deflection.

The pitching moment due to the horizontal tail is

$$C_{m_t} = -V_t C_{N_t} \quad (8)$$

where V_t is a *ratio* of volumes

$$V_t = \frac{L_t A_t}{L A_p}. \quad (9)$$

Ignoring any moment contribution due to a low center of gravity (CG), requiring that the tail moment balance the wing/body moment gives

$$V_t = \frac{C_{m_{wb}}}{C_{N_t}} \quad (10)$$

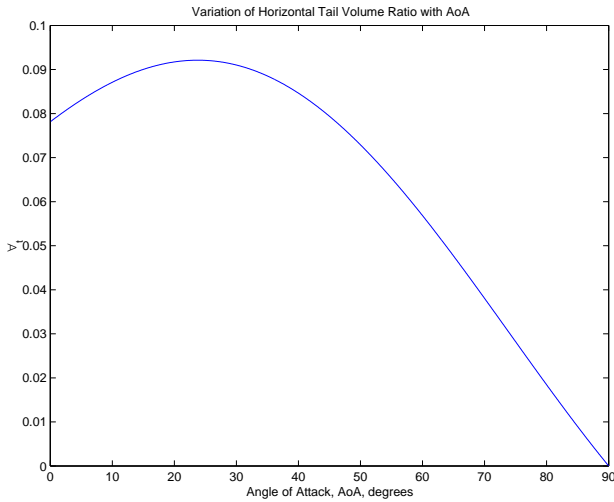


Fig. 5. Relation between angle of attack and tail volume ratio

Using (2) and (6) one obtains the following relationship between angle of attack and the horizontal tail volume ratio:

$$V_t = \frac{\pi}{8} f \left(0.222 + \frac{0.283}{\sin \alpha} \right) \left(\frac{1}{\gamma^2} + \gamma^2 - 1 \right) \sin 2\alpha \cos \frac{\alpha}{2} \quad (11)$$

Equation (11) can be used to size the tail for the “worst case scenario” in which the CG coincides with the CB. Using parameters for the wingless VTMAUV as an example, one obtains the curve shown in Fig. 5. Choosing the value of V_t greater than the peak value, which occurs around $\alpha = 24^\circ$, will ensure that the tail counteracts the destabilizing wing/body moment throughout the full range of speeds and angles of attack.

Ensuring that there is sufficient control authority to maintain a given pitch attitude, however, is a separate issue. For conventional streamlined AUVs, the CG is below the CB for static tilt stability. At some minimum speed, the stern planes are unable to overcome the stabilizing CG moment. Rather than increase the tail volume ratio (9) to decrease this minimum speed, we consider moving the CG itself.

III. DYNAMIC MODELING

To develop a dynamic model, define a second reference frame, fixed in inertial space, by the orthonormal triad (x_I, y_I, z_I) with z_I pointing in the direction of the local gravity vector. The vehicle position is given by the inertial vector $\mathbf{X} = [x, y, z]^T$ which extends from the origin of the inertial frame to the origin of the body frame. The attitude can be described using the conventional XYZ Euler angles $\Phi = [\phi, \theta, \psi]^T$ as defined, for example, in [2]. The body translational and angular velocity are $\mathbf{v} = [u, v, w]^T$ and $\boldsymbol{\omega} = [p, q, r]^T$, respectively.

The kinematic equations are

$$\begin{pmatrix} \dot{\mathbf{X}} \\ \dot{\Phi} \end{pmatrix} = \begin{pmatrix} \mathbf{J}_1(\phi, \theta, \psi) \mathbf{v} \\ \mathbf{J}_2(\phi, \theta) \boldsymbol{\omega} \end{pmatrix} \quad (12)$$

where

$$\mathbf{J}_1 = \begin{pmatrix} c\theta c\psi & s\phi s\theta c\psi - c\phi s\psi & c\phi s\theta c\psi + s\phi s\psi \\ c\theta s\psi & c\phi c\psi + s\phi s\theta s\psi & -s\phi c\psi + c\phi s\theta s\psi \\ -s\theta & s\phi c\theta & c\phi c\theta \end{pmatrix}$$

and

$$\mathbf{J}_2 = \begin{pmatrix} 1 & s\phi t\theta & c\phi t\theta \\ 0 & c\phi & -s\phi \\ 0 & s\phi/c\theta & c\phi/c\theta \end{pmatrix}.$$

In the expressions above, “s” represents the sine function, “c” represents the cosine function, and “t” represents the tangent function.

Now let the body vector \mathbf{r}_p denote the position of the moving mass particle relative to the origin of the body frame. The velocity of the mass particle relative to inertial space (but expressed in the rotating body frame) is

$$\mathbf{v}_p = \mathbf{v} + \boldsymbol{\omega} \times \mathbf{r}_p + \dot{\mathbf{r}}_p. \quad (13)$$

Assuming that the point mass is constrained to move parallel to the vehicle’s longitudinal axis, only the first component of

the vector \mathbf{r}_p is free to vary under the influence of a control force. We therefore define $r_p = \mathbf{e}_1 \cdot \mathbf{r}_p$ where $\mathbf{e}_1 = [1, 0, 0]^T$.

To develop the dynamic equations, first define the 7×7 generalized inertia matrix for the body/particle system

$$\mathbb{I}_{b/p} = \begin{pmatrix} \mathbf{J}_b - m_p \hat{\mathbf{r}}_p \hat{\mathbf{r}}_p & m_b \hat{\mathbf{r}}_{cg} + m_p \hat{\mathbf{r}}_p & m_p \hat{\mathbf{r}}_p \mathbf{e}_1 \\ -m_b \hat{\mathbf{r}}_{cg} - m_p \hat{\mathbf{r}}_p & m\mathbf{I} & m_p \mathbf{e}_1 \\ -m_p \mathbf{e}_1^T \hat{\mathbf{r}}_p & m_p \mathbf{e}_1^T & m_p \end{pmatrix}.$$

In the expression above, the operator $\hat{\cdot}$ is used to convert a vector into a skew-symmetric matrix that satisfies $\hat{\mathbf{x}}\mathbf{y} = \mathbf{x} \times \mathbf{y}$ for vectors \mathbf{x} and \mathbf{y} . Also, \mathbf{J}_b represents the 3×3 rigid body inertia matrix and \mathbf{I} represents the 3×3 identity matrix.

The generalized *added* inertia matrix is

$$\mathbb{I}_a = \begin{pmatrix} \mathbf{J}_a & \mathbf{D}_a & \mathbf{0} \\ \mathbf{D}_a^T & \mathbf{M}_a & \mathbf{0} \\ \mathbf{0}^T & \mathbf{0}^T & 0 \end{pmatrix}.$$

where \mathbf{J}_a represents added inertia, \mathbf{D}_a represents inertial hydrodynamic coupling, and \mathbf{M}_a represents added mass. Each of these matrices is 3×3 . Added mass and inertia arise from potential flow theory; the associated ‘‘inertial forces’’ account for the effort required to accelerate the fluid around the body as it moves.

The total generalized inertia matrix is the sum of the generalized body/particle system inertia and the generalized inertia due to the fluid, $\mathbb{I}_{sys} = \mathbb{I}_{b/p} + \mathbb{I}_a$. The matrix \mathbb{I}_{sys} is positive definite and depends on the vehicle geometry and mass distribution and on the density ρ of the ambient fluid.

The total body angular momentum \mathbf{h}_{sys} , the total body linear momentum \mathbf{p}_{sys} , and the along-track point mass momentum p_p are defined as follows:

$$\begin{pmatrix} \mathbf{h}_{sys} \\ \mathbf{p}_{sys} \\ p_p \end{pmatrix} = \mathbb{I}_{sys} \begin{pmatrix} \boldsymbol{\omega} \\ \mathbf{v} \\ \dot{r}_p \end{pmatrix}. \quad (14)$$

With these definitions, the dynamic equations are [10]

$$\begin{aligned} \dot{\mathbf{h}}_{sys} &= \mathbf{h}_{sys} \times \boldsymbol{\omega} + \mathbf{p}_{sys} \times \mathbf{v} + \mathbf{m}_{ext} \\ \dot{\mathbf{p}}_{sys} &= \mathbf{p}_{sys} \times \boldsymbol{\omega} + \mathbf{f}_{ext} \\ \dot{p}_p &= u_p + f_{p_{ext}} \end{aligned}$$

where \mathbf{m}_{ext} and \mathbf{f}_{ext} represent external moments and forces applied to the vehicle, respectively. These include gravitational effects (weight and buoyancy), viscous flow effects (such as lift and drag and angular rate damping), and the vehicle thrust. The term u_p in the last equation represents a control force acting along the moving mass track; the term $f_{p_{ext}}$ represents other along-track external forces, such as gravity and friction. To implement moving mass control, one may choose the control input to cancel the relative motion of the mass induced by the vehicle itself and to servo the mass to its desired position.

Steady motion at constant depth requires that \mathbf{v} , z , and r_p remain constant and that $\boldsymbol{\omega} = \mathbf{0}$. From these requirements, the following equilibrium conditions must hold:

$$\mathbf{m}_{ext} = (m\mathbf{I} + \mathbf{M}_a) \mathbf{v} \times \mathbf{v} \quad (15)$$

$$\mathbf{f}_{ext} = \mathbf{0}. \quad (16)$$

Define the terms

$$\begin{aligned} m_T &= m_b + m_p - m_{buoy} \\ N_T &= N_{wb} + N_t \\ A_T &= A_{wb} + A_t. \end{aligned}$$

Thus, $m_T g$ represents the submerged weight of the vehicle, N_T represents the total hydrodynamic normal force, and A_T represents the total hydrodynamic axial force. From the free body diagram in Fig. 3, the condition (16) requires

$$m_T g = N_T \cos \theta - A_T \sin \theta + T \sin \theta. \quad (17)$$

A horizontal force balance gives

$$0 = T \cos \theta - A_T \cos \theta - N_T \sin \theta.$$

Solving for the thrust required to maintain constant speed gives

$$T = A_T + N_T \tan \theta \quad (18)$$

Substituting (18) into (17) yields

$$\begin{aligned} m_T g &= N_T \cos \theta - A_T \sin \theta + A_T \sin \theta + N_T \tan \theta \sin \theta \\ &= N_T \cos \theta + N_T \tan \theta \sin \theta \\ &= N_T \cos \theta (1 + \tan^2 \theta) \\ &= N_T \sec \theta. \end{aligned}$$

Solving for the total normal force gives

$$N_T = m_T g \cos \theta.$$

Normalizing and solving for the dynamic pressure gives

$$P_{dyn} = \frac{m_T g \cos \theta}{C_N(\alpha) \mathbb{A}_r} \quad (19)$$

where $C_N(\alpha)$ is given by (5). Noting that $\theta = \alpha$ for constant depth flight, equation (19) relates the equilibrium pitch angle to the dynamic pressure. The minimum achievable equilibrium speed is

$$V_{min} = \min_{\theta} \left[\frac{2 m_T g \cos \theta}{\rho C_N(\theta) \mathbb{A}_r} \right]^{\frac{1}{2}}.$$

The equilibrium moving mass position can be obtained by choosing r_p such that, at the equilibrium pitch angle, the moment due to $m_p g$ balances the hydrodynamic moment (4) and the residual CG moment due to the fixed vehicle weight $m_b g$.

IV. EXPERIMENTAL PROOF OF CONCEPT

This section describes design and field trials of a one degree of freedom MMA built for use with the VTMAUV. The goal is to demonstrate the use of a MMA to lower the minimum speed for a streamlined AUV by supplementing the control authority of servo-actuated tail fins.

A. Actuator Design

The MMA was designed to mimic the size and shape of a YSI CTD sensor, which is a standard payload for the VTMAUV. Attached below the vehicle, the MMA provides passive roll stability by lowering the vehicle's CG. The VTMAUV supplies the MMA with 5 volts DC power. The actuator is controlled serially using simple position commands. The command set is the set of integers from 0 through 60, with 0 corresponding to the rearward-most mass position and 60 corresponding to a forward-most position.

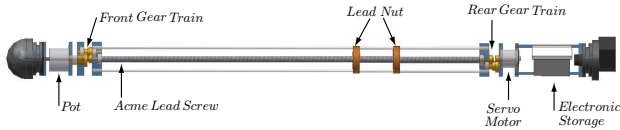


Fig. 6. Components of the MMA.

The layout of MMA components is shown in Fig. 6. The mass moves along an Acme $\frac{1}{4}$ -inch lead screw with a pitch of $\frac{1}{3}$ -inch per turn. The lead screw is driven through a custom-designed gear assembly by a high torque servomotor located at the rear of the actuator. The integrated servo potentiometer was replaced by an equivalently rated 10-turn potentiometer which is slaved to the lead screw at the front of the actuator through another gear assembly. Two brass lead screw nuts travel along the lead screw; a pair of anodized aluminum rails prevent the lead screw nuts from rotating, ensuring a smooth linear motion. A bolted assembly of brass weights, sandwiched between the lead screw nuts, serves as the moving mass. The amount of movable mass can be varied to change the net buoyancy of the MMA. For the experiments described in this section, the amount of movable mass was chosen to give the combined VTMAUV/MMA assembly a net buoyant force of 1.5% of the dry weight. The moving mass accounted for roughly 15% of the total vehicle weight. With a full travel distance of approximately 8 inches, the MMA provides 1 inch of longitudinal movement of the vehicle CG, a significant amount considering the scale of the vehicle.

B. Experimental Results

The MMA was attached to the VTMAUV and ballasted so that the assembly sits level in the water with the moving mass centered at position 30. To verify that the VTMAUV could operate over the entire range of moving mass positions, the vehicle was commanded to swim at its nominal speed of 1 m/s and to maintain a depth of 1.5 meters in a series of experiments for which the moving mass was fixed at various locations. (In all experiments, a separate PID feedback loop actuated the fins to maintain the specified depth.)

Control, depth, and attitude histories were recorded for experiments corresponding to seven mass locations. One such data set is shown in Fig. 7. The data suggest near-equilibrium flight. The time histories were averaged to yield the equilibrium approximations shown in Table I. A front view of the tail fin configuration for the VTMAUV is shown in Fig. 8. The

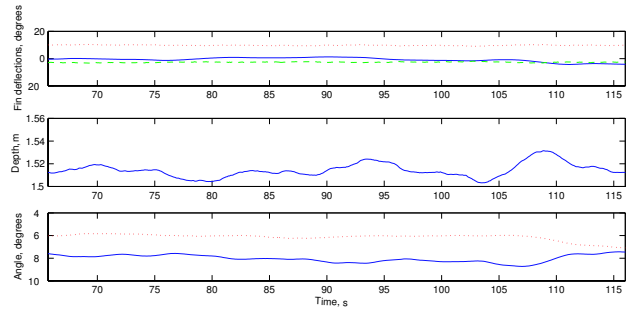


Fig. 7. Dynamic data taken with MMA at position 30. (In the top plot, the solid line represents Fin_a , the dashed line represents Fin_b , and the dotted line represents Fin_c . In the bottom plot, the solid line represents pitch angle and the dotted line represents roll angle.)

TABLE I
EQUILIBRIUM CONDITIONS AT MASS LOCATIONS

MMA Location	Depth	Pitch	Roll	Fin_a	Fin_b	Fin_c
2	1.5°	-11.3°	-4.5°	10.1°	11.7°	-4.6°
10	1.5°	-9.8°	-4.5°	5.8°	8.2°	-1.1°
20	1.5°	-8.3°	-5.1°	4.3°	4.0°	3.1°
30	1.5°	-7.9°	-6.2°	-0.8°	-2.7°	9.8°
40	1.5°	-6.5°	-5.4°	-1.5°	-5.8°	12.9°
50	1.5°	-5.7°	-6.7°	-3.6°	-8.3°	15.4°
60	1.5°	-5.6°	-8.6°	-6.6°	-11.2°	18.3°

apparent discrepancy between the Fin_a and Fin_b data shown in Fig. 7 is due to the constant roll moment required to counter the roll moment induced by the propeller. As can be seen in

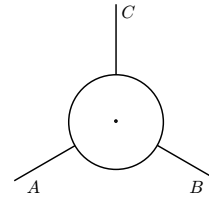


Fig. 8. VTMAUV fin orientation, viewed from the front.

Fig. 9, the PID-controlled fins compensate for the changing gravitational moment as the moving mass travels forward from its rearward-most location.

The vehicle is trimmed so that, for a moving mass location of 30, the CG is longitudinally aligned with the CB. Smaller (more rearward) mass locations generate a nose-up gravitational moment which must be countered by the tail fins to maintain a nose-down attitude. Larger (more forward) mass locations require less moment of the tail fins up to the point where the nose-down attitude exceeds the trim condition, at which point the fins must generate a nose-up moment. At this critical mass location, the fins become unnecessary as the entire equilibrium pitch control moment is generated by the MMA. This observation is particularly important for control at lower speeds, where the fins might be incapable of generating the necessary equilibrium pitch control moment.

The vehicle was next programmed to maintain depth with the moving mass at its rearward-most position, allowing suf-

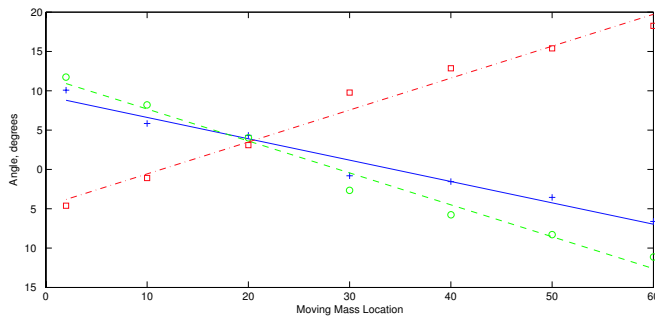


Fig. 9. Equilibrium fin locations with commanded MMA locations. (The solid line represents a linear fit to the Fin_a data points '+'. The dashed line represents a linear fit to the Fin_b data points 'o'. The dash-dotted line represents a linear fit to the Fin_c data points '□'.)

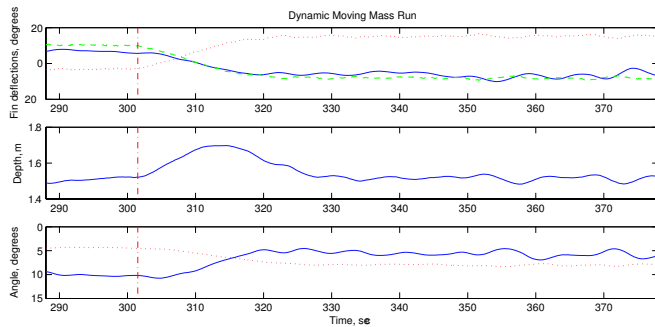


Fig. 10. Vehicle response to slewing the moving mass from its full rearward to its full forward location. The transition begins at $t = 301.5$ seconds. (In the top plot, the solid line represents Fin_a , the dashed line represents Fin_b , and the dotted line represents Fin_c . In the bottom plot, the solid line represents pitch angle and the dotted line represents roll angle.)

ficient time to achieve steady state, after which the mass was slewed to its forward-most location. Again the vehicle was programmed to travel at its design speed of 1 m/s. The control, depth, and attitude histories are shown in Fig. 10, where the vertical dashed line indicates the beginning of the moving mass transition. As the mass moves forward, the vehicle pitches nose-down and dives slightly. Eventually, once the mass has reached its forward-most position, the PID depth controller brings the vehicle back to its specified depth. Initially, the tail fins are deflected leading edge up to generate a nose-down moment. The local lift generated by the fins is therefore upward and must be opposed by additional down force on the vehicle hull. Thus, the trim pitch angle is more negative at the beginning of the experiment. As the tail fins adjust to the forward-moving CG, they generate less upward force and, eventually, begin generating downward force. As a result, the equilibrium pitch angle becomes less negative because less down force must be generated by the hull.

From one point of view, the dynamic data shown in Fig. 10 illustrate the VTMAUV depth controller's ability to reject steady pitch disturbances. Viewed another way, the data illustrate the MMA's effectiveness at generating a pitch control moment. Moreover, because this control moment is independent of vehicle speed, the MMA should also be effective for depth control at low speeds.

V. CONCLUSION

Streamlined AUVs are typically trimmed to be somewhat buoyant or heavy in water. To maintain depth, they must generate a constant hydrodynamic force which requires that they swim at a constant pitch angle. Although tail fins are the typical mechanism for generating this control moment, they become ineffective at low speeds. To enable an existing AUV to travel at lower speeds, one may easily incorporate a modular moving mass actuator. In some cases, it may also be advantageous to include a fixed wing.

In addition to static analysis that provides actuator and wing sizing guidelines, this paper describes the design of a one degree of freedom moving mass actuator module and preliminary experiments using the Virginia Tech Miniature AUV. The results illustrate the effectiveness of a moving mass actuator at generating control moments. Planned experiments should further demonstrate the actuator's ability to control an AUV at an otherwise uncontrollably low speed.

ACKNOWLEDGMENT

The authors gratefully acknowledge the sponsorship of the National Science Foundation, under Grants CMS-0133210 and IIS-0238092, and the Office of Naval Research, under grants N00014-01-1-0588, N00014-03-1-0444, and N00014-05-1-0780.

REFERENCES

- [1] R. E. Davis, C. C. Eriksen, and C. P. Jones. Autonomous buoyancy-driven underwater gliders. In G. Griffiths, editor, *Technology and Applications of Autonomous Underwater Vehicles*, volume 2, chapter 3. Taylor and Francis, 2002.
- [2] Thor I. Fossen. *Guidance and Control of Ocean Vehicles*. John Wiley and Sons, West Sussex, England, 1994.
- [3] A. S. Gadre, J. J. Mach, D. J. Stilwell, and C. E. Wick. Design of a prototype miniature autonomous underwater vehicle. In *IEEE/RSJ Intelligent Robotics and Systems*, pages 842–846, Las Vegas, NV, 2003.
- [4] J. G. Graver. *Underwater Gliders: Dynamics, Control, and Design*. PhD thesis, Princeton University, 2005.
- [5] B. Hobson, M. Kemp, and A. Leonessa. Integration of a hovering module on to the Morpheus AUV: Application to MCM missions. In *MTS/IEEE OCEANS 2002*, pages 207–209, Biloxi, MS, 2002.
- [6] Sighard F. Hoerner. *Fluid-Dynamic Lift*. Hoerner Fluid Dynamics, Brick Town, NJ, 1975.
- [7] S. A. Jenkins, D. E. Humphreys, J. Sherman, J. Osse, C. Jones, N. Leonard, J. Graver, R. Bachmayer, T. Clem, P. Carroll, P. Davis, J. Berry, P. Worley, and J. Wasyl. Underwater glider system study. Technical report, Office of Naval Research, 2003.
- [8] Leland H. Jorgensen. A method for estimating static aerodynamic characteristics for slender bodies of circular and noncircular cross section alone and with lifting surfaces at angles of attack from 0° to 90° . Technical Report NASA TN D-7228, Ames Research Center, Moffett Field, Calif. 94035, April 1973.
- [9] N. Kato and I. Tadahiko. Guidance and control of fish robot with apparatus of pectoral fin motion. In *Proc. International Conference on Robotics and Automation*, pages 446–451, Leuven, Belgium, May 1998.
- [10] C. A. Woolsey. Reduced Hamiltonian dynamics for a rigid body/mass particle system. *Journal of Guidance, Control, and Dynamics*, 28(1):131–138, 2005.
- [11] C. A. Woolsey and N. E. Leonard. Stabilizing underwater vehicle motion using internal rotors. *Automatica*, 38(12):2053–2062, 2002.